Chapter 1

Introduction

Chapter 1
Introduction

1.1 General Statement and Scope of the Work

The evolution of the earth during the last 3.0 Ga has witnessed dramatic changes in size, relative position, and geographic distribution of the continents (Rogers, 1996; Aspler and Chiarenzelli, 1998). The assembly and fragmentation of supercontinents had profound effects on the earth's atmosphere, hydrosphere, and climate, and as a consequence, on the global sedimentary and stratigraphic records (Worsley *et al.*, 1986; Young, 1988).

The Proterozoic supracrustal sequences are important for understanding the origin and evolution of the continental crust, its composition, the earth's surface processes, and the sediment provenance (Eriksson and Soegaard, 1985; McLennan and Taylor, 1991; Eriksson and Cheney, 1992). In reality, however, the Proterozoic siliciclastic basins are often bracketed by rare, imprecise stratigraphic data and nonuniform characters of the earth processes (Haddox and Dott, 1990; McCormick and Grotzinger, 1993; Whipple and Trayler, 1996). This often leads to the presentation of poorly constrained basin models (Shaw, 1964; Altermann and Nelson, 1998).

In spite of all these limitations, much interest has centered on the stratigraphic, structural, and sedimentological aspects of the Proterozoic sedimentary basins (Brookfield, 2008). The origin and evolution of many such basins and basin-fill successions are poorly understood, not because the records of the thick Proterozoic supracrustal successions are not widespread in the geological history, but because of the absence of the present day analogs (Shaw, 1964).

The Indian shield behaved coherently since Archean-Proterozoic amalgamation and as a result, a number of unmetamorphosed Proterozoic sedimentary successions developed during the Proterozoic (Naqvi and Rogers, 1987; Radhakrishna, 1987; Kale and Phansalkar, 1991; Rogers, 1993; Rogers and Santosh, 2004; Naqvi, 2005). The sedimentological studies of the Proterozoic sedimentary successions over the past years have concentrated mainly on the identification of the sedimentary precursor rocks, their structures, and the paleocurrent directions (Naqvi and Rogers, 1987). A detailed investigation of the outcrop analogs along with the sedimentary structures appear to be the most effective means for predicting the stratal geometries and the basin models.

The unmetamorphosed sedimentary sequences within the Proterozoic basins of India occur in multiple unconformity-bounded sequences, and are characterized by a high degree of commonality with respect to the lithological and lithofacies associations and depositional environments. The sequences are dominated by fluviatile-shallow marine clastics and carbonates, occurring as facies sheets that extend over thousands of square kilometers and are arranged in an aggradational facies architectural order. These are commonly described as layer-cake stratifications (Radhakrishna, 1987). It is believed that the primordial basins were formed within the cratonic rifts that developed along the crustal weak zones and later rapidly evolved into small and large basins (Naqvi and Rogers, 1987).

The depositional systems of the thick wedges and sheets of mature clastics of the Paleoproterozoic Kolhan basin (Fig. 1.1) (~2.1-2.2 Ga, Saha, 1994; Balasubrahmanyan, 2006) have been analyzed in a general way. They have been considered to be similar in many respects with the ca. 2.0-1.9 Ga Waterberg Group preserved in the Middelburg basin developed on the Kaapvaal craton, South Africa (Eriksson *et al.*, 2006) and with the ca. 3.2-3.0 Ga Bababudan Group developed on the Dharwar craton, India (Balasubrahmanyan, 2006), suggesting a possible Indo-African connection during the Archean – Proterozoic era. The clastic wedges are best developed in the eastern part of the basin, whereas in the central and western part, the succession is characterized by extensive sheet-like deposits of mature sandstones and shale. The method of process oriented analysis of outcrop analogs have been used to reconstruct the depositional systems and stratigraphy and develop a depositional model of sedimentation at the early stage of the basin extension. This study documents the depositional structures, lithostratigraphic and lithofacies relationships, paleocurrent and paleohydraulic geometries, sedimentation dynamics, basin-fill architecture, and symmetricity of a Paleoproterozoic fluvial (braided river) system developed around Chamakpur-Keonjhargarh region (Dalabehera and Das, 2007, 2008; Dalabehera, 2009a-c; Dalabehera and Das, 2009a-b; Dalabehera *et al.*, 2009) within the Kolhan basin, Orissa (Saha, 1994; Bose, 2009).

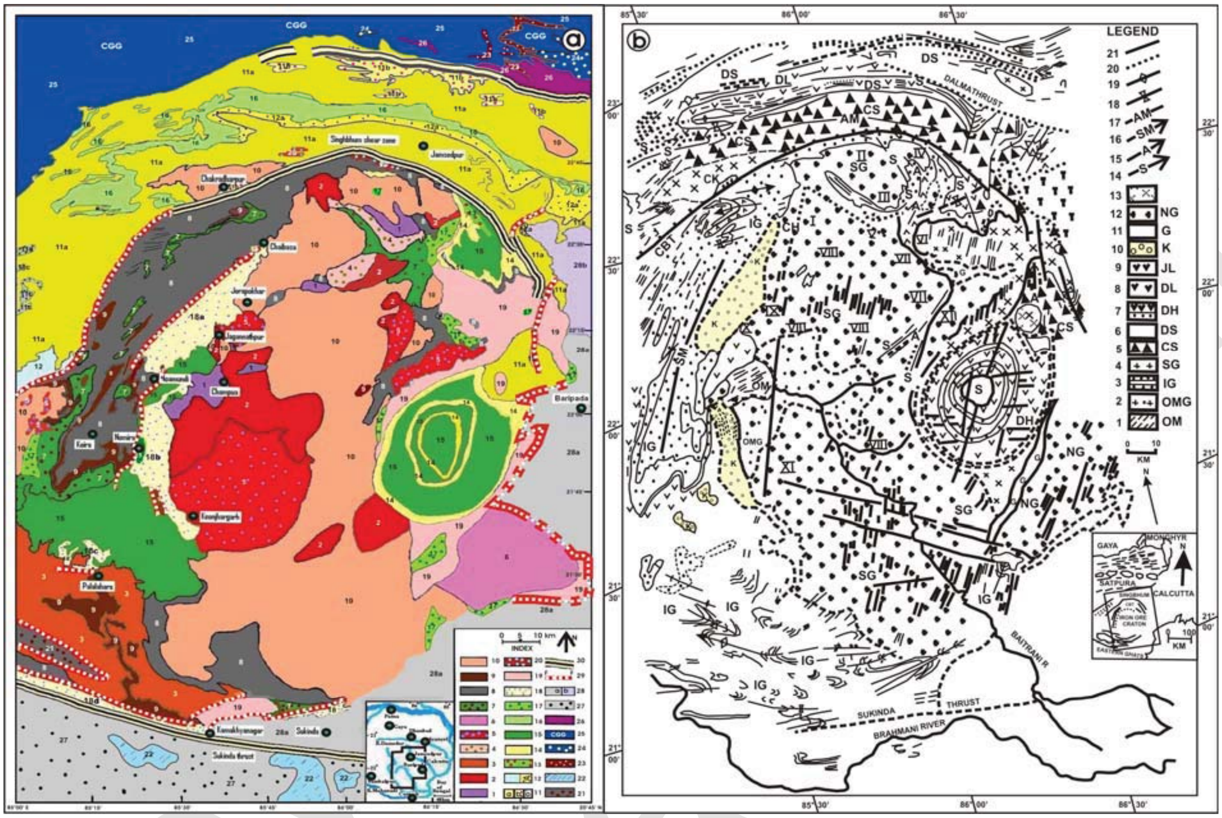

Fig. 1.1: (a) Generalized geological map of the Singhbhum-North Orissa region (Saha, 1994).
Legend: 1-Older Metamorphic Group; 2-Older Metamorphic Tonalite-gneiss; 3-Pala Lahara gneiss; 4-Singhbum granite-phase I; 5-Singhbum granite-phase II and xenolith dominated areas of Bonai granite; 6-Nilgiri granite; 7-Iron Ore Group lavas, ultramafics; 8-Iron Ore Group shales, tuffs, phyllites; 9-BHJ, BHQ and sandstone-conglomerate of Iron Ore Group; 10-Singhbhum granite-phase III; Bonai granite; Chakradharpur granite; 11-Singhbhum Group (a) pelites, psammipelites (b) mafic bodies (c) carbon phyllite; 12-Singhbhum Group quartzites; (a) quartzites-pelites; 13-Dhanjori Group (unclassified); 14-Quartzite-conglomerate-pelite of Dhanjori Group; 15-Dhanjori-Similipal-Jagannathpur-Malangtoli lavas; 16-Dalma lavas; 17-Proterozoic gabbro-anorthosite-ultramafics; 18-Kolhan Group and equivalents (a. Chaibasa-Noamundi basin, b. Chamakpur-Keonjhargarh basin, c. Mankarchua basin, d. Sarapalli-Kamakhyanagar basin); 19-Mayurbhanj granite; 20-Soda granite, Arkasani granophyre, Kuilapal granite, Alkaline granite; 21-Charnockite; 22-Khondalite; 23-Amphibolite enclaves (within CGG); 24-Pelitic enclaves within CGG; 25-Chhotanagpur granite gneiss (CGG); 26-Porphyritic member of CGG; 27-Gondwana sediments; 28-Alluvium, Tertiaries; 29-Fault; 30-Thrust fault.
(b) Geotectonic-cum-geological map of Singhbhum, Keonjhar, Mayurbhanj District, and adjacent region based on ERTS (LANDSAT) imagery and ground data, showing linears, geological boundaries, axial traces of folds of different generations, Copper Belt Thrust (CBT) and Sukinda Thrust (Sarkar and Saha, 1977).
Legend: 1-OM, Older Metamorphic group; 2-OMG, Older Metamorphic gneiss; 3-IG, Iron Ore Group lavas, BHJ and shales; 4-SG, Singhbhum granite, the individual magmatic units denoted by Roman numerals I-XII; 5-CS-Chaibasa Formation; 6-DS, Dhalbhum Formation; 7-DH, Dhanjori sandstone-conglomerate and lava; 8-DL-Dalma lava; 9-JL, Jagannathpur lava; 10-K, Kolhan Group; 11-G, Gabbro-anorthosite; 12-NG, Nilgiri granite possibly related to Singhbhum granite; 13-Granites related to Singhbhum orogenic cycle; 14-Synform of first generation; 15-Antiform of first generation; 18-Synform of second generation; 19-Antiform of second generation; 20-Thrust and Wrench fault; 21-Linears and formation boundaries; CH-Chaibasa; CK-Chakradharpur.

Interpreting the depositional environment of the thick Proterozoic Kolhan sequence was difficult because of (a) the absence of body fossils which could provide tell-tale evidence of the depositional environment and (b) the absence of land vegetation, which has a profound influence on the precipitation, run-off, and sediment yield (Dalabehera and Das, 2009b). The lines of evidence adopted to determine the environment of deposition for the Kolhans were grain size, petrography, sandbody geometry, lithofacies association, type, scale, abundance and the directional attributes of sedimentary structures, fining and coarsening upward cycles, and large-scale lateral accretion surfaces (Long, 1978).

The study also demonstrates that inspite of (a) the high rate of formation of the accommodation space, (b) moderate-low slope, and (c) high availability of coarse-fine material, braided streams developed (Dalabehera and Das, 2009b). Further the study also demonstrates that where the slope and discharge values were below the critical limit, a significant proportion of suspended load:bed load ratio always existed, which otherwise is favorable for the formation of meandering streams (Schumm, 1968; Cotter, 1978; Long, 1978; Rust, 1978; Blum and Tornqvist, 2000).

Precambrian fluvial systems lacked the influence of rooted vegetation (Blum and Tornqvist, 2000) and were probably characterized by flashy surface runoff, low bank stability, broad channels with abundant bed load, and faster rates of channel migration. As a result, a braided fluvial style developed (Blum and Tornqvist, 2000). These braided river systems which were active under highly variable paleoclimatic conditions, perhaps were more widespread. Aeolian deflation of fine fluvial detritus does not appear to have been prevalent. With the onset of large cratons during the Neoarchaean – Paleoproterozoic era, very large, ephemeral-braided river systems developed (Rust, 1978). The ca. 2.1-2.2 Ga Kolhan Group is a reflection of this process and was deposited largely by alluvial/braided-fluvial processes within fault-bounded, possibly pull-apart type depositories (Saha, 1994).

1.2 Previous Work

Jones (1934) included members of the Kolhan Group as part of his Iron Ore Series. Dunn (1940) used the term ‘Kolhan Group’ for a sequence of unmetamorphosed sedimentary formation overlying the Singhbhum granite and later Dunn and Dey (1942) correlated the Kolhan Group with the Dhanjoris of eastern Singhbhum. The existence of the Kolhan Group in the Chamakpur-Keonjhargarh basin was under debate for a long time (Mukhopadhyay, 1988). Four different views published with regard to the status of the sedimentaries of this basin are: (a) the sedimentary horizon is older than the Jagannathpur volcanics and the Iron Ore Group (Misra, 1961), (b) the horizon is an outlier in the down-buckled area of the Iron Ore basin (Sarangi and Acharya, 1970), (c) the horizon is equivalent to the Dhanjori and Daitari-Tomka Iron Formation (BIF-2 of Acharya, 1976, 1984), and (d) the horizon is either equivalent to the Bonai Group (Mazumder, 1996) or is to be correlated with the Koira Group (Ramakrishnan and Vaidyanadhan, 2008).

Field studies at the contact of the Kolhan orthoquartzites with the Iron Ore Group (IOG) of rocks, both against the main basin as well as at the Gandhamardhan-Suakati outlier of Banded Iron Formations, show that the horsted block was uplifted in between the Kolhans in the east and the Malangtoli lavas in the west (Saha, 1994). The presence of pebbles and blocks of the BHJ and granite in the basal sandstone indicates that the Kolhan Group is post-IOG and Singhbhum granite (Dalabehera and Das, 2009b). At the Deo River section (north of Jagannathpur), the base of the Kolhan ferruginous sandstone (dipping 5°-15° west) overlies the steep-dipping IOG tuffs which is intruded by the leucocratic Singhbhum granite (Saha, 1994). The presence of sills of Newer Dolerites shows that the Kolhans are older than the dolerites. Acharya (2009) opines that there are no dolerite dykes in the Kolhan Groups. Hence, the dykes should be considered older than the Kolhans in the stratigraphic table of Saha (1994)**.**

The formation of Kolhan basin then may have been initiated during the large withdrawal of basaltic magma, which caused extensive dyke formation and thermal subsidence (Mahadevan, 2002, p.252). All these confirm the existence of the Kolhan basin (equivalent to the Purana basin of Central and South India) and therefore the basin must have a stratigraphic entity as pointed out by Saha (1994) (Table 1.1). Barring local investigations (Ghosh and Chatterjee, 1994), detailed sedimentological studies in the Kolhan basin around Chamakpur-Keonjhargarh have not been made before.

Table 1.1: Simplified Chronostratigraphic Succession for the Singhbhum Craton, Eastern India (Saha *et al.*, 1988; Mukhopadhyay, 2001; Balasubrahmanyan, 2006)

Newer Dolerite dykes and sills	ca. 1.6 - 0.95 Ga
Mayurbhanj Granite	ca. 2.1 Ga
Gabbro – anorthosite – ultramafics	
Kolhan Group	ca. 2.1 - 2.2 Ga
~~**Unconformity**~~~~~~~~~~~~~~~~~	
Jagannathpur / Malangtoli and Dhanjori – Simlipal Lavas, Quartzite – Conglomerate (Dhanjori Group)	ca. 2.3 Ga
Pelitic and arenaceous metasediments with mafic sills (Singhbhum Group)	ca. 2.3 - 2.4 Ga
~~**Unconformity**~~~~~~~~~~~~~~~~~	
Singhbhum Granite Phase III (SBG B)	ca. 3.1 Ga
Epidiorites (intrusives) Iron Ore Group (IOG, volcano-sediments)	
~~**Unconformity**~~~~~~~~~~~~~~~~~	
Singhbhum Granite Phase I and II (SBG A), Nilgiri Granite, Bonai Granite	ca. 3.3 Ga
Older Metamorphic Group (OMG) and Older Metamorphic Tonalite-gneiss, folding and metamorphism	ca. 3.4-3.5 Ga
Older Metamorphic Tonalite-gneiss (OMTG)	ca. 3.77 Ga
Older Metamorphic Group (OMG)	ca. 4.0 Ga

The present study is in agreement with the views of Saha (1994). It is believed that the siliciclastic rocks of the region belong to Kolhan Group. The reasons cited are as follows.

(i) The similarity in the architectural pattern of the different lithofacies of the area when compared to those of the type area of the Kolhan basin ***(Chaibasa - Noamundi basin, Fig. 1.1a).***

(ii) The trend of outcrops around the western part of the Singhbhum granite massif and their persistent low westerly dip values suggest a close similarity in the tectonic and stratigraphic framework.

(iii) The variation in the lithology across and within a basin does not necessarily indicate different stratigraphic entity but merely represents the lithofacies variation of the same unit; the changes in the lithofacies characters are dependent on sedimentary processes, sediment supply, climate, tectonics, sea-level changes, water chemistry, and bathymetry.

(iv) The siliciclastic rocks of the study area and that of the type area represent contemporaneous lithofacies variation of the same sandstone unit; gravity tectonics and lateral displacement during sedimentation caused local facies changes.

(v) The composition of the lithic grains and pebbles within the coarse and medium grained siliciclastics shows that the sediments have been derived from the Singhbhum granite and Iron Ore Group of rocks.

(vi) The heavy mineral concentrates show a similarity in their abundance and type with those of the type area (Chaibasa-Noamundi basin, Saha, 1994) of the Kolhan basin.

(vii) The Kolhan basin is shallow in nature and probably had a wide extension than what is envisaged; paleocurrent studies do indicate a uniformity in slope and a progressive deepening of the basin towards north and west.

1.3 Geodynamic Setting of the Proterozoic Kolhan Basin

The Singhbhum craton in eastern India is composed of Archean granitoids forming the nucleus rimmed by a Proterozoic mobile belt to the north and east (Sarkar and Saha, 1977; Saha, 1994). To the west and southwest of the Singhbhum granite, the Kolhan Group is preserved as a linear belt extending for 80-100 km with an average width of 10-12 km (Fig. 1.1), revealing deposition of Kolhan sediments in narrow and elongated depressions. It is believed that the Kolhans were deposited in the intracratonic basins developed within the Singhbhum-Orissa Iron Ore craton (Fig. 1.1c), with a general NNE-SSW alignment and were controlled by the trend of the Iron Ore synclinorium (Saha, 1994). There is also a strong asymmetry in the vertical basin-fill succession that has given rise to lithofacies variations within the Kolhans.

The Kolhans are now preserved as isolated outliers that spread over four detached basins (Fig. 1.1a) (Saha, 1994): (a) Chaibasa - Noamundi basin, (b) Chamakpur - Keonjhargarh basin, (c) Mankarchua basin, and (d) Sarapalli - Kamakhyanagar basin. The 2.1-2.2 Ga (Saha, 1994) mixed siliciclastic-carbonate Kolhan Group (Saha *et al.*, 1988; Mukhopadhyay, 2001) represents the youngest Precambrian stratigraphic unit in Singhbhum geology (Saha, 1994; Mukhopadhyay, 2001; Bose, 2009).

The Kolhans in general show low (5°-10°) westerly dip, and cover an approximate area of 800 km^2 and unconformably overlie the Singhbhum granite to the east and show a faulted contact with the Iron Ore Group of rocks to the west (Saha, 1994). Locally, a pyrophyllitic shale layer (10 m thickness) is present in between the Singhbhum granite and the Kolhans (Saha, 1994). The study area is around Chamakpur - Keonjhargarh (Long. 85°20'-85°35' E **;** Lat. 21°35'-22°10' N) (Fig. 1.2a) covering an area approximately 370 km^2 (length : 50-55 km ; width : 6-8 km).

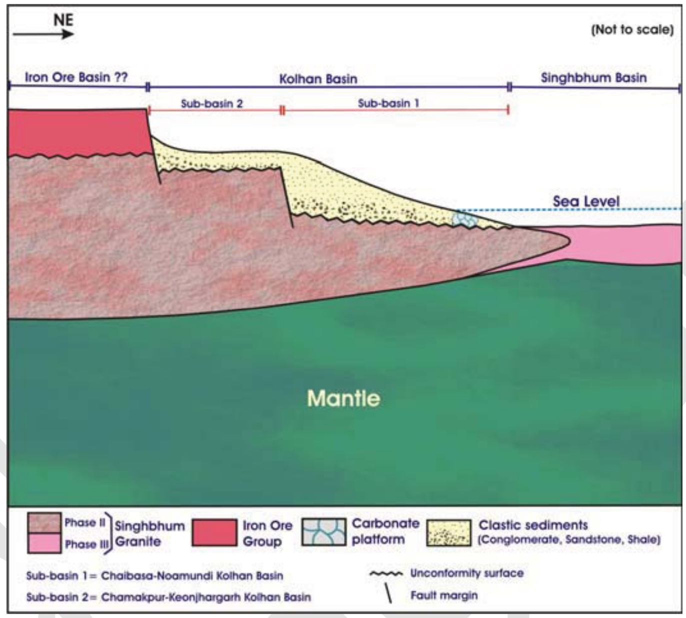

Fig. 1.1: (c) Schematic model for the transgressive Kolhans developed in a riftogenic setting (not to scale).

Geophysical studies across the Kolhan basin along two transects (BB' and AA'A'', Figs. 1.2b-c, Verma *et al.*, 1984) show a gravity high due to the presence of Iron Ore synclinorium and the Kolhan basin (Verma *et al.*, 1984). The basinal thickness of the Kolhan sediments is approximately 1.5 km (Verma *et al.*, 1978, 1984; Saha *et al.*, 1988; Saha, 1994).

1.4 Objectives and Organization of the Work

The entire plan of the work was divided into various phases for carrying out detailed sedimentological studies in the study area. The major objectives of this work have been as follows:

- To identify the generic components of the basinal sediments preserved within the Proterozoic Kolhan basin.

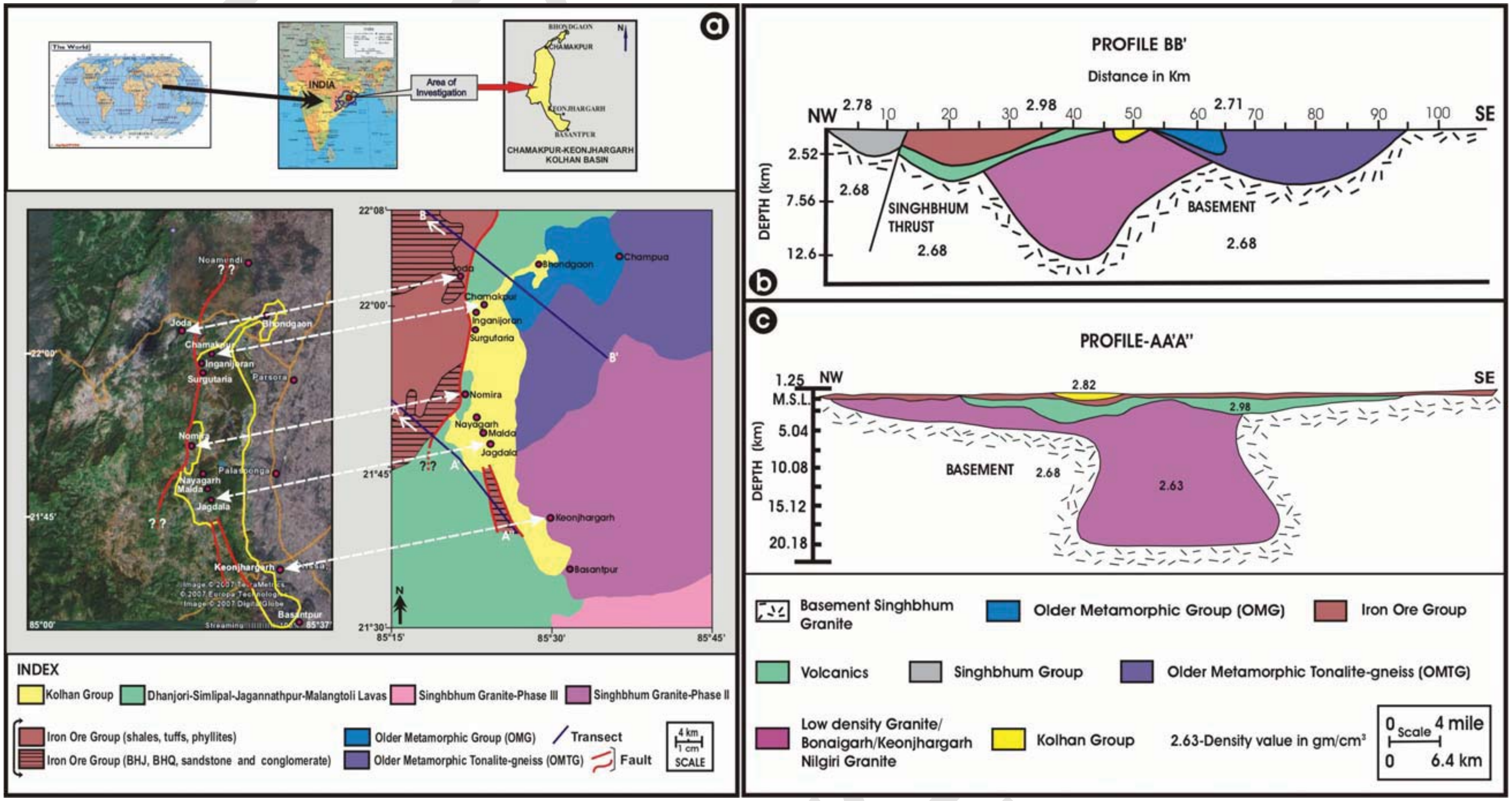

Fig. 1.2: **(a)** Satellite imagery (left) (Google Earth, 2007) and the geological map of Kolhan basin (right) around Chamakpur-Keonjhargarh region (Saha, 1994). AA'A'' and BB' are the section lines across the basin. **(b)** Profile AA'A'' across the Keonjhargarh granite, IOG rocks, volcanics, and Kolhan Group. **(c)** Profile BB' across Singhbhum Group, IOG rocks, volcanics, Kolhan Group, and Older Metamorphics based on gravity data (Verma *et al.*, 1984). The thickness of the Kolhan basin is around 1.5 km (Note : The Singhbhum Group has not been shown in the geological map of Kolhan basin).

- To model the depositional framework and the general continuity of the sedimentation pattern in the light of geological setting, field-based primary sedimentary structures, lithofacies geometries, petrofacies analyses, sediment geochemistry, paleocurrent, paleohydraulic, and provenance studies.
- To study the spatial and temporal variations between the lithounits and establish the facies changes along and across the basin.
- To establish the paleoflow intensities and directions within the basin from the paleohydraulic and paleocurrent studies.
- To establish the pattern of lineage between the facies transition, facies build-up, and facies correlation across the basin through Markov chain and Cross-association analysis.
- To establish the three dimensional facies architecture of the Proterozoic Kolhan basin in the study area.

The work distribution is appended below.

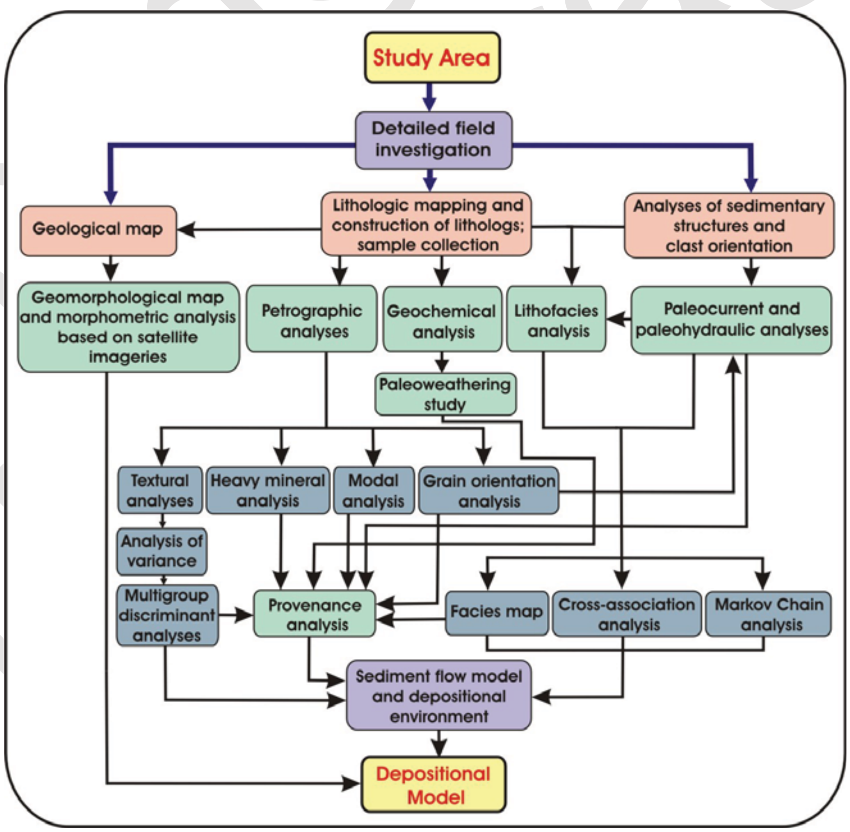

Flow chart depicting the steps used to carry out the present work

1.5 Methods of Study

1.5.1 Field Work and Field Methods

Litholog Constructions

Fieldworks were carried out to describe and characterize the lithounits of the Kolhan basin. Vertical stratigraphic sections along and across the River Baitarani were studied and exposures were mapped. At each exposure, the different lithounits were studied and were identified on the basis of their bed geometries, gross lithologies, and sedimentary structures. The textural and the structural aspects of the lithounits observed in the outcrops were then clubbed into six lithofacies for better representation. The identity of each lithofacies was based on the presence of a set of primary textures and structures (Selley, 1970, 1976). For all field geological mapping, the Survey of India (1982) Toposheets (Nos. 73 G/5, 73 G/6, 73 G/9, 73 G/10, 73 F/8, and 73 F/12) were used on a working scale of 1:50,000.

Paleocurrent Analyses

Paleocurrent data were recorded in course of the structural and lithofacies mapping over most of the accessible outcrops in the area. Multistage methods of hierarchical sampling (Krumbein and Graybill, 1965; Davis, 2002) were followed for measuring azimuths of directional data. In many cases, paleocurrents were directly measured (Allen, 1982) from trough and tabular cross-bed axis, sole mark, and groove mark. The grain orientations (apposition fabric) were also measured (Spotts, 1964; Harms, 1979; Allen, 1982) to determine the paleocurrent direction. The grain orientation data have been used as references for matching data obtained from other approaches. Necessary tilt corrections were done following standard methods outlined by Pettijohn and Potter (1964), Ramsay (1967), Parks (1970a-b), Phillips (1971), and Potter and Pettijohn (1977). The details of paleocurrent analyses are given below.

- **From trough and tabular cross-bedding**

Trough cross-stratification is the most abundant, accurate, and efficient paleocurrent direction indicator. However, exposures in which trough-axes can be measured are rare. Two methods were used for the determination of paleocurrent directions from the more common exposure types: the use of three-dimensional exposures of oblique sections through individual trough limbs, and two-dimensional exposures of sets of trough cross-strata. Three-dimensional exposures of trough limbs can be measured and treated statistically on a stereographic plot to determine the average trough-axis orientation. In two-dimensional exposures, characteristic asymmetry of the basal scour surface and truncation of foreset laminae can aid in estimation within about 25 degrees of paleocurrent direction (Pettijohn and Potter, 1964; Potter and Pettijohn, 1977; De Celles *et al.*, 1983; Nemec, 1988).

- **From other directional structures of non-depositional nature**

Paleocurrents were also recorded from erosional structures such as sole mark and groove mark. Most of these give the current trend (Pettijohn and Potter, 1964; Selley, 1988; Friedman *et al.*, 1992).

If more than one tool mark were found on the bedding plane, as many as possible were measured and the mean was computed (about 3% of the bedding planes contain groove marks). In some cases, distinct sets cross-cutting each other were also observed, in which case separate means were calculated. In few locales of the study area, about 4.3% of 567 bedding planes with groove marks show two distinct crossing sets and 1.2% show three sets.

- **From grain orientation**

The azimuths of the long axes of the ellipsoidal detrital grains tend to align themselves parallel to the direction of flow of the currents (Taira and Lienert, 1979). Analyses of apposition fabric of 457 grains (4.00-0.13 mm size) from fifty oriented samples have been done following the method of Dapples and Rominger (1945). The long axes of the rectangles with least projection and the broad ends of the teardrop shaped grains have been determined from the grain outlines. The azimuth between flow direction of each grain and magnetic north was measured in a clockwise direction. Individual grain measurements have been grouped into twelve classes following the method suggested by High and Picard (1971). The total number and percentage of grains measured obtained in each dodecant were plotted on polar graph paper (High and Picard, 1971).

1.5.2 Laboratory Investigation

Geomorphological Analysis

GTOPO30 (Global 30 Arc-Second Elevation Data Set) of the study area were obtained from the United States Geological Survey's (USGS) EROS data centre (http://eros.usgs.gov/products/elevation/gtopo30/gtopo30.html). The hypsographic data were then analyzed using Golden Surfer (version 7.0) software package and the 3d Digital Elevation Model (DEM) of the study area was obtained to understand the topography of the area. The geological and geomorphological maps of the study area were prepared with the help of field data and geocoded IRS-1D, LISS III satellite data (2001), available with ORSAC, Bhubaneswar.

Thin Section Granulometric and Petrographic Analyses

Sixty-eight samples from six lithofacies (medium to coarse-grained and texturally submature - mature) were collected from the study area. As no carbonates were recorded in thin sections, no efforts were made to use staining techniques used for carbonates. However, thin sections were washed with hydrofluoric acid to remove all carbonates if any.

- **Granulometric analyses**

The granulometric analyses of the rocks from the thin sections have been carried out following standard methods (Folk and Ward, 1957; Friedman, 1961, 1967). Statistical variants were determined following methods of Passega (1957, 1964), Sahu (1964, 1983), Sevon (1966), Greenwood (1969), and Davis (2002). The analyses of shape, roundness, and packing of the siliciclastic grains have been done following the methods of Powers (1953), Kahn (1956), Anger (1963), and Pettijohn (2004).

Roundness analysis: The roundness values of more than 200 detrital quartz grains have been measured and classified into different roundness intervals (Powers, 1953; Pettijohn, 2004). On an average, the ratio between the high and low sphericity detritals is about 7:3. If n_l, n_2, n_3, n_4, n_5, and n_6 are the number frequencies corresponding to six roundness classes, then the $\text{Average Roundness} = \dfrac{n_1m_1 + n_2m_2 + n_3m_3 + \ldots.. + n_6m_6}{Sn}$

where $Sn = n_l + n_2 + n_3 + n_4 + n_5 + n_6$ and $m_l, m_2, m_3,....., m_6$ denote the mid points of each roundness class interval.

Packing density (Pd) analysis: Packing density is a measure of the amount of space occupied by the grains in a given area within the thin section.

$$Pd = (m\sum_{i=1}^{n} gi/t).100\ ;\ 0 < \sum_{i=1}^{n} gi \leq t/m$$

$\sum_{i=1}^{n} gi$ = sum of all the grain intercept values in a given traverse, where Pd = packing density, m = micrometric correction factor, t = total length of the traverse.

Packing proximity (Pp) analysis: Packing proximity is a unit packing property which is related to the presence or absence of contacts between grains.

$Pp = (q / n) \times 100\ ;\ 0 \leq q \leq n$; where q = number of grain to grain contacts, n = total number of contacts.

- **Petrographic and modal analysis**

Primary structures and textural features are very well preserved in the sedimentary rocks and metamorphism is negligible. Thus, the prefix 'meta' has been omitted here and the original sedimentary nomenclature has been used. The general petrographic characterization of the conglomerates-sandstones has been retained and focused. The more labile samples collected from the vertical sections include quartz arenite, sublitharenite, and subarkose-arkose. Many of these rock sections contain significant amount of secondary porosity and authigenic clay that have formed at the expense of the feldspars and the rock fragments. Hence, it is likely that some of these samples were originally quartz-rich subarkose and feldspathic-lithic arenite.

Modal analyses of the rock thin sections were done by Gazzi-Dickinson point counter with the count of a minimum of 200 framework grains per thin section. Matrix problems were minimized during counting by tabulating only those masses of the matrix that displayed obvious grain boundaries or other criteria of pseudomatrix (Dickinson and Suczek, 1979). The Gazzi-Dickinson point counting method (Dickinson and Suczek, 1979; Basu, 1985) minimizes compositional variation due to grain size differences by assigning sand sized grains within rock fragments to their own category rather than to that of the rock fragments. This method was used not only to confirm that the defined petrologic trends are unrelated to variable grain size but also to provide data that can be plotted in tectonic provenance discrimination diagrams (Dickinson and Suczek, 1979; Dickinson, 1985). All calculations for determining the volume percentages of minerals were done following standard method outlined by Dickinson and Suczek (1979).

- **Heavy mineral analysis**

For heavy mineral analysis, 250 gm fractions from each sandstone samples were initially mechanically reduced by steel mortar to an intermediate size followed by porcelain mortar and pestle to fine size fractions (Folk, 1966). The ASTM –60 to +80, –80 to +100, and –100 to +120 fractions (Folk, 1966, 1980) were separated by sieving. The heavy minerals in each of these fractions were subsequently separated following the techniques of Argast and Donnelley (1986), Stewart (1986), and Lindholm (1991) using Jeffrey's centrifuge tubes with bromoform (sp.gr. 2.85) as the heavy liquid medium. The abundance of heavy minerals in ASTM –60 to +80 mesh size crushed samples, in most cases, is around 2% by weight, which is good enough (Folk, 1966). The separated heavy minerals were mounted on microscopic slides for study under the microscope and their semi-quantitative estimation was carried out using a point counting method (Stewart, 1986; Lindholm, 1991).

Chemical Analysis (X-Ray Fluorescence Spectrometry)

Samples of six lithofacies of Kolhan were analyzed for their major element oxides by X-ray Fluorescence Spectrometry. Twenty samples were washed, air dried and then fragmented to about 1 cm size and divided into 8 parts by coning and quartering and one part each (about 250 gm) was pulverized to -200 mesh size to a homogeneous powder in the WC Planetary Mill. Care was taken at each stage of crushing, coning-quartering, and pulverizing to avoid contamination. One gram each of the powdered sample was fused with 10 grams of lithium tetraborate with a PHILIPS Mini Fuse at a temperature of 1000^{o}C and quenched to obtain a homogeneous bead of 27 mm diameter. The beads were used for measurement of ten major element oxides. Standards were selected to cover the appropriate range in the major element concentrations. Fused beads were prepared of the same standards. A PHILIPS PW 2404 X-Ray Fluorescence Spectrometer with a 4 kW Rh

X-ray tube was used for the major element analyses. The SUPERQ software package supplied with the spectrometer was used for calibration and routine analyses.

Paleohydraulic Analysis

The mean cross-bed set thickness computed from 146 measurements in the field was found to be 0.11 m. The channel sinuosity, channel width, width/depth ratio, meander wavelength, channel slope, bankful depth, flow velocity, flood stage velocity, flow depth, stream power, clast flow velocity, and Froude number were calculated following standard methods (Hjulström, 1939; Schumm, 1963; Leopold *et al.*, 1964; Carlston, 1965; Simons *et al.*, 1965; Allen, 1968; Malde, 1968; Southard, 1971; Miall, 1976; Middleton and Southard, 1978; Barrett and Fitzegerald, 1985; Sengupta, 1994). The various governing equations used have been given in Appendix A.

1.5.3 Numerical and Computational Methods

Software packages used for the statistical analyses and graphical representations were GEOrient 9.2, Grapher 6.0, LogPlot 7.0, MATLAB 7.4, MS Excel 2007, ORIGIN 7.5, ROCKWORKS 2006, SIGMAPLOT 10.0, SPSS 12.0, Surfer 7.0, STATISTICA 8.0, SYSTAT 7.0, SEDFLUX 2008, SEDPAK 2008, and SEDSIM 2007. Adobe-Photoshop 8.0, ArcGIS 9.0, AutoCAD 2006, CorelDRAW 11.6, and MS Paint 5.1 were the drawing toolkits used for drawing maps, log sections, and field sketches.

Statistical Analyses of Oriented Data

For a better understanding of the local and regional paleoflow patterns, the area was divided into a number of sections of equal dimension (approx. 4 km^2) using hierarchical sample design method (Olson and Potter, 1954). The paleocurrent measurements (both directional structures and grain orientations) were obtained from approximately twenty-one exposures. The bulk data for the entire area were grouped at 30° class intervals for preparing circular histograms (Nemec, 1988). The azimuth of the directional structures and preferred grain orientations were then statistically tested (Curray, 1956; Krumbein and Graybill, 1965; Wood and Wood, 1966). The paleoflow directions were calculated following the vector resultant method (Curray, 1956; Krumbein and Graybill, 1965) and the circular arithmetic mean method (Wood and Wood, 1966). The Turkey chi-square (χ^2) test of significance was calculated following the methods of Harrison (1957), Rusnak

(1957), Middleton (1965, 1967), and Davis (2002). The computation sheet for χ^2 tests is partially shown in Table B.1 (Appendix B).

- **Vector method**

(1) The mean vector may be calculated by any of the two methods.

i. $\tan\theta = \sum n_0 \sin\theta_i / \sum n_0 \cos\theta_i$ (Davis, 2002)

ii. $\theta = 0° + \alpha$ if $C \geq 0$ (Curray, 1956)

$= 180° + \alpha$ if $C \leq 0$

where $\tan \alpha = S/C$

$C = \sum N\cos\theta_i / (\sum \cos^2\theta_i)^{1/2}$

$S = \sum N\sin\theta_i / (\sum \sin^2\theta_i)^{1/2}$

θ = azimuth of resultant vector

θ_i = mid point of *ith* class interval in degrees

n_o = number of observation per interval

n_e = expected number of observation per interval

(2) The resultant vector θ, is an estimate of the central tendency. The significance of θ at a particular level for two degrees of freedom has to be matched with the standard value (Davis, 2002, p. 607-608, Table A.4).

$\chi^2 = C^2+S^2$

(3) The magnitude of the resultant vector

$r = \{(\sum n_o \sin\theta_i)^2 + (\sum n_o \cos\theta_i)^2\}^{1/2}$ (Curray, 1956).

(4) The magnitude of resultant vector in terms of percent

$L = (r\times100) / \sum n_o$, where n_o is observed frequency.

(5) To find significant concentration of the observed frequency distribution in the class interval, the standard deviation (S) is calculated by the formula $S^2 = (n_o - n_e)^2/n-1$, i.e. $S = \{(n_o-n_e)^2/n-1\}^{1/2}$ (Dixon and Massey, 1957).

Concentration are significant in polymodal distribution if $n_o \geq (n_e+s)$.

- **Circular arithmetic mean method**

Various methods have been proposed for the 2d and 3d display of the grain orientation and other vectorial data (Jizba, 1971; Agterberg, 1974). Wood and Wood (1966) have given an algebraic solution of the treatment of the orientation data. It extracts all arithmetic means of the data and is independent of the choice of the origin. The computational procedure for circular arithmetic means (θm) has been given in Table B.2 (Appendix B). The linear arithmetic mean ($\overline{Y}$) and the function Ψ and Ψ' are calculated as : $\overline{Y} = \sum_{j=1}^{N} y_j f_j / n$; $\Psi = \overline{Y} + (360^o/n)\ k \ (\mathrm{mod}\ 360^o)$; $\Psi' = \Psi_j + (180^o/n)\ f_{j+1}\ (\mathrm{mod}\ 360^o)$ (Table B.2, Appendix B).

Since N (number of class interval) is an *even number* in the present investigation, the interval file 'I' (Table B.2, Appendix B) starting at the bottom opposite Y_N or Y_{12} may be calculated as: $I_N = (Y_{N/2}, Y_{N/2+1})$.

The circular arithmetic means (θm values) were calculated as follows:

When Ψ lies within the open interval 'I' and is also opposite, then Ψ is a mean θm; whenever Ψ' lie on the value of the right hand end point of the interval 'I' and is also opposite, it is the mean θm. The mean with minimum positive deviation is generally taken as the preferred orientation or vector resultant direction (Davis, 2002).

As a confirmation, the data were again tested using the methods of Curray (1956), Batschelet (1981), and Davis (2002). The resultant paleocurrent vector $(\overline{\theta}V)$, vector strength $(\overline{R})$, 95% confidence interval, circular standard deviation (S), variance (S^2), and probability of randomness (p) were calculated for each sector and also for the entire study area:

$$\overline{\theta}V = \tan^{-1}\sqrt{\frac{\sum \sin\theta}{\sum \cos\theta}} \qquad \text{...(1.1) (Davis, 2002)}$$

$$\overline{R} = \frac{1}{n}\sqrt{(\sum \sin\theta)^2 + (\sum \cos\theta)^2} \qquad \text{...(1.2) (Davis, 2002)}$$

$$95\%\ \text{confidence level} = \pm\frac{180}{\pi}\times 1.96\times\frac{1}{\sqrt{n\overline{R}k}} \qquad \text{...(1.3) (Davis, 2002)}$$

$$S = \frac{180}{\pi}\sqrt{2(1-\overline{R})} \qquad \text{...(1.4) (Batschelet, 1981)}$$

$$p = e^{-(\overline{R})^2 n} \qquad \text{...(1.5) (Curray, 1956)}$$

where n = number of observations

θ = direction of concavity of the trough-axis in degrees from north

k = concentration parameter …(1.6) (Davis, 2002)

Multigroup Discriminant Analysis of Textural and Structural Data

- **Markov chain and Sediment trend analysis**

Markov chain analysis (Davis, 2002) was carried out to analyze the order of sequence and transition in the facies lineage. The principles and methods used have been given in Appendix C. Sediment transition path and sediment trend analysis were established following the concept of McLaren (1981).

- **Cross-association analysis**

Cross-association analysis has been done to compare the twelve vertical sequences (Davis, 2002, p. 248). The distribution profile of the coefficient of cross-association between the two equivalent sequences, both showing non-Markovian character, is asymptotic in nature. Initially, the twelve lithologs were paired on the basis of dispersal patterns. The more unique characteristics that the paired sections share, the greater the probability that the correlation is stratigraphically correct. In each pair the data set of the second vertical log have been moved past against the data set of the first log from bottom upwards, one set at a time, and the degree of correspondence between the overlapped segments at each position was calculated. The process was repeated till the bottom set of the second log coincided with the topmost set of the first log (Davis, 2002). At each matching position, the matching ratio (number of matches to number of comparisons) was computed, which was used as an index of similarity of the two chains at the overlapping position. The ***associatograms*** were obtained by plotting the matching position versus matching ratio. The significance of the matching ratio was determined by chi-square test (Davis, 2002). The chi-square test is used to test the null hypothesis (H_0) that the two sets of data formed random sequences and the observed number of matches and mismatches were not greater than expected from the two random sequences of equivalent composition.

Let the two vertical sequences with m possible categories be designated as chain 1 and chain 2. If the number of observations in the k^{th} state of chain 1 is X_{1k}, the total length of chain 1 is $n_1 = \sum_{k=1}^{m} X_{1k}$. In chain 2, there are also *m* categories each with X_{2k} observations giving a total length of chain 2 as $n_2 = \sum_{k=1}^{m} X_{2k}$. The probability of match is the sum of the products of each of the *m* categories in the two chains divided by the product of chain length i.e., $P = \frac{\sum_{k=1}^{m} X_{1k} X_{2k}}{n_1 n_2}$ and $\chi 2 = \frac{(O - E)^2}{E} + \frac{(O' - E')^2}{E'}$ (where P = probability of matches, O=observed number of matches, O'= observed number of mismatches, E = expected number of matches, E' = expected number of mismatches, the chi-square ($\chi 2$) has one degree of freedom having the critical value 3.84).

- **Linear discriminant functional analysis**

Discriminant functions display the true degree of distinctness of multivariate samples and also condense information relative to a large number of characteristics (Greenwood, 1969). The potential for discriminant analysis was tested using size-frequency statistics from a series of random samples selected from the study area. The discriminant functions of Sahu (1964) and Sevon (1966) have been used (Appendix D) to delineate sedimentary environment from sets of variables.

- **Multigroup discriminant analysis**

The identity of a facies can be done through linear discriminant analysis, which takes into account a large number of sediment parameters in terms of their lithologies, structures, and textures simultaneously and allots certain numerical indices to each facies (Greenwood, 1969). The unrestricted use of any single variable is often alleged because of its possible interaction with a number of other variables (Sahu, 1983). Therefore, using the multivariate statistical analysis with large number of variables, a meaningful uniformitarianism can be achieved with minimum error.

The problem of discriminating sedimentary environments on the basis of measurable sediment parameters can be resolved through multivariate statistics (Rao, 1952; Sahu, 1964, 1983; Greenwood, 1969; Colley and Lohnes, 1971; Bennett and Bowers, 1977; Ross and Lee, 2006; Hartmann, 2007). The procedure generates discriminant function(s) (for a minimum of two groups) based on linear combinations of the predictor variables that provide the best discrimination between the groups. The functions are generated from sample of cases for which the group membership is known, which can then further be applied to new cases for determining the predictor variables for the unknown group membership.

The sediment textures (Friedman and Sanders, 1978; Folk, 1980) and primary sedimentary structures are the variables that provide information about the medium, mode of transport, and the energy conditions at the time of deposition, and are therefore useful markers of interpreting the depositional environment. These variables have been taken as the independent variables in the discriminant analysis studies.

A multivariate grouping procedure has been used for assigning individual variables to distinct groups or facies, and standard methods (Greenwood, 1969; Davis, 2002) have been applied to differentiate the different lithofacies on the basis of the above variables with the help of modern software package (SPSS 12.0). Multigroup discriminant analysis was done for the six lithofacies (GLA, GSD, SSD, PLSD, RSD, and TLSD) using both textural parameters and sedimentary structures as variables on a *64 X 72 matrix*. Each group was treated five times in combination with other five groups leading to a total combination of fifteen. The variable having maximum recurrence with minimum significance value was taken as the dominant discriminating variable (Greenwood, 1969; Davis, 2002).

Wilks' lambda (λ), a parameter which is often used for determining the statistical significance of the output variables, and is done through the 'F test' (Greenwood, 1969). The smaller the value of λ , the more important role the independent variable plays for the generation of the discriminant function. Each discriminant function is characterized by an eigenvalue, which in turn reflects the importance of the dependent variables. For two-group discriminant analysis, there is one discriminant function and one eigenvalue, which accounts for the total variance in the distribution system (Davis, 2002). The larger the eigenvalue, the more of the variance within the dependent variable is explained by that function. Thus the discriminant function assesses the variables and further classifies its role and importance within a multigroup system.

The canonical correlation (R^*, Greenwood, 1969) is a measure of the association between the groups formed by the dependent variable and the determined discriminant function. When R^* is zero, there is no relation between the groups and the function. When the numerical value of canonical correlation is high (close to 1), there is a high correlation between the discriminant functions and the groups under study. One can only understand the significance of each function for discrimination between the groups (e.g., R^*=1.0 means all the variables can be used for discrimination study).

1.6 Contributions of the Research Student

The scholar has reported for the first time the presence of paleofluvial activities in the Kolhan basin. A depositional model for the Chamakpur-Keonjhargarh region has been developed accordingly. The paleochannel patterns could serve as repositories for ancient placer deposits of gold and uranium. The change in the fluvial system has been microscaled under two broad stratigraphic patterns and the reasons for doing so have been focused. However, the basin architecture, spatial and temporal constraints within the basin, the framework of the basement, the basement heterogeneity, and the thermal history have to be examined in depth to develop a coherent geodynamic model for the complete process modeling of the Kolhan basin.